Custom Fit Non-Invasive Ventilation Mask with Microclimate Monitor: Preliminary Study

S. Morad[1,*] and S. Lindsay[2]

[1]University of East London, London, E16 2RD, UK
[2]Sandwell & West Birmingham NHS Trust, Hallam St, West Bromwich B71 4HJ, UK
Email: s.morad@uel.ac.uk (S.M.); shaun.lindsay1@nhs.net (S.L.)
*Corresponding author

Abstract—**Mask and interface design have been emphasized in previous research in relation to Non-invasive Ventilation (NIV) and pressure ulcer prevention. A number of variables contribute to necrosis, but critical research has shown that the skin-mask interface is the most important. The goal of this study is to determine whether preexisting ventilation mask designs can be modified in order to improve clinical outcomes. A Custom-Fit ventilation Mask (CFM) was created using 3D scanning and printer technology. A disposable, custom-fit cushion has been fabricated in order to integrate with a pre-existing mask. A mask is equipped with embedded sensors that measure the microclimate between the skin and the mask as precisely as possible. Real-time data is plotted and monitored for critical conditions and to identify other key features. A preliminary Temperature-Humidity (T-H) monitoring of the skin-mask interface shows fluctuation trends that could potentially induce PUs. However, there is a less sensitive reaction in the original mask test.**

Keywords—**embedded sensors, microclimate monitor, pressure ulcers, ventilation mask**

I. INTRODUCTION

Pressure Ulcers (PUs) are common in Non-invasive Ventilation (NIV) users because symptoms can appear as early as 4-6 hours after starting continuous ventilation [1]. The primary cause of facial pressure ulcers has been identified as prolonged mechanical pressure [2]. Friction, on the other hand, causes shear stresses at the skin-mask interface, which damage the epidermis. Furthermore, skin movement caused by ill-fitting masks and interface gaps increases these stresses, resulting in frequent cases of skin ischemia and necrosis [3]. When a Custom-Fit Mask (CFM) is designed to match the contours of the face, the interface becomes smaller, reducing displacements and the associated shear stresses. Furthermore, a uniform redistribution of pressure along facial tissue means that prominent bony landmarks like the bridge of the nose and chin will be less likely to suffer damage that is commonly seen during treatment [4].

The mask microclimate is defined as the skin Temperature and Humidity (T-H) at the skin-cushion interface, and it has been shown to influence the rate and severity of PUs [2]. As a result, these are the parameters selected for analysis, and the best place to do so is at this interface. Temperature and Relative Humidity (RH) both exacerbate the effects of mechanical pressure on the skin by weakening its structural and physiological capabilities to withstand it [5].

Excessive moisture on the epidermis raises the coefficient of friction [6], while the epidermis softens, making it more vulnerable to damage [7, 8]. Low humidity, on the other hand, reduces water content in the stratum corneum, lowering tensile strength and flexibility [9]. Furthermore, the proper use of a humidified ventilation system may help prevent NIV-induced airway dryness and promote the transport of pulmonary secretions [10]. Also, the utility of measuring the temperature at PU sites was noted by Yilmaz and Gunes [11], whereby increases in exogenous heat raise vasodilation and, therefore, oxygen consumption, carbon dioxide production, and waste product excretion at the local site, worsening the effect.

As a result, maintaining optimal T-H levels throughout treatment is critical for dissipating loads through deformation and maintaining normal barrier function. Because the CFM improves the seal and thus the T-H at the interface, the improved mask will benefit from microclimate monitoring.

There are only a few studies that explain patient-specific NIV mask designs. Tsuboi *et al.* [12] and Lanza *et al.* [13] show promising results with their masks in terms of increasing patient comfort and reducing leakage, but the design is made with manual molding methods, such as maxillofacial elastomer in the latter, preventing the clinical benefits that non-contact methods could provide. Han *et al.* [14] was the first to use 3D scanning technology to create a custom-fit mask; however, this was merely a pilot study and not intended for the NIV. A study aimed at lowering the cost of clinical applications attempted to use Computer Numerical Control (CNC) for manufacturing. The results were more encouraging, with a better fit [15]. Wu *et al.* [16] used 3D printing with partial success due to the addition of a silicone layer on some of their masks, but this eventually led to intolerable leaks. Furthermore, Magnetic Resonance Imaging (MRI) was used to collect data in this study, reducing its cost-effectiveness in a clinical setting. Previous research has yielded promising results; however, no study has yet to incorporate low-cost scanning and 3D printing into a sensing system to truly optimize CFM potential.

A. Determining the Threshold Values

Although acceptable microclimate values are unknown, reasonable suggestions have been made [17]. Previous studies were used to estimate dangerous levels and the monitor's subsequent threshold limits.

Temperatures above 35 °C have been shown to reduce the mechanical stiffness and strength of the stratum corneum while determining temperature limits [18]. Each 1 °C increase after that results in a 13% increase in metabolic demand, further wearing down the relevant tissue by reducing the available energetic resources in the PU area [19].

Skin temperature in the NIV, on the other hand, should not fall below the average room temperature of 22 °C because some degree of warm air is required for alveolar gas exchange [20].

Engebretsen *et al.* [21] examined a plethora of studies in order to determine the risks of an unstable microclimate. According to the paper, a normal RH value is between 40% and 70%; thus, the lower RH threshold is set to 40%. However, a high level of humidification is required for NIV, and at 100% RH, the strength of the stratum corneum is reported to be 25 times weaker than at 50% RH [22], indicating an upper RH threshold of 100%.

B. Existing Mask Types

Mask design is critical in NIV; Kramer *et al.* [23] reported that NIV fails in 18% of cases due to the discomfort associated with many conventional mask types. The most common example (70%) is the oronasal mask. Nonetheless, the nasal mask is frequently used (25%) and nasal prongs are mostly used in neonates (5%). Other NIV masks, such as total face masks and helmets, are available, but they are only used in specialized treatments [24]. Many studies highlight the reasons for oronasal mask popularity, such as [25], which describes how oronasal masks are the most tolerable during NIV in patient surveys, compared to nasal prongs and nasal masks. Nasal masks provide the most benefits for the majority of clinical needs. However, their limited usage could undoubtedly be affected by the low efficacy of this mask type, requiring additional chin straps to prevent mouth leaks [26].

II. MATERIALS AND METHODS

A. Development of the Cushion

Data for the face mesh is collected using an Occipital 3D Structure Sensor. The mesh file is processed in SolidWorks using 3DtoScan to remove small artefacts. The mask and facial mesh were designed to be integrated into the cushion design, allowing the sensor to be placed closer to the skin. The surface tool was used in conjunction with the curve tool to add the properly contoured edge to the cushion's face side; mirroring the curve also helped maintain symmetry for a more aesthetically acceptable outcome (Fig. 1).
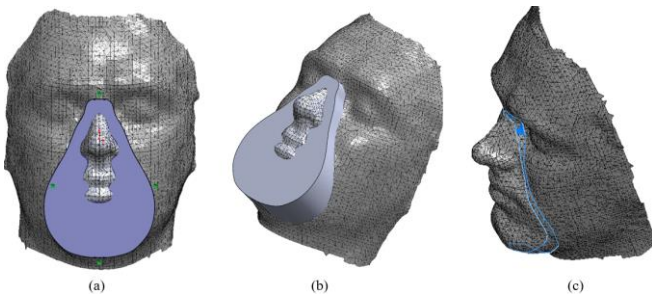

Fig. 1. Projecting the mask profile. (a) Sketch of mask shape (b) Project shape to surface (c) Result.

The humidity and temperature sensor (SHT85) is placed at the skin-mask interface to effectively monitor the microclimate (Fig. 2). A single extrusion between the two meshes was used to recreate the entire model. Non-essential edges were also smoothed down, and the model's aesthetics were improved through mesh refinement with Blender and
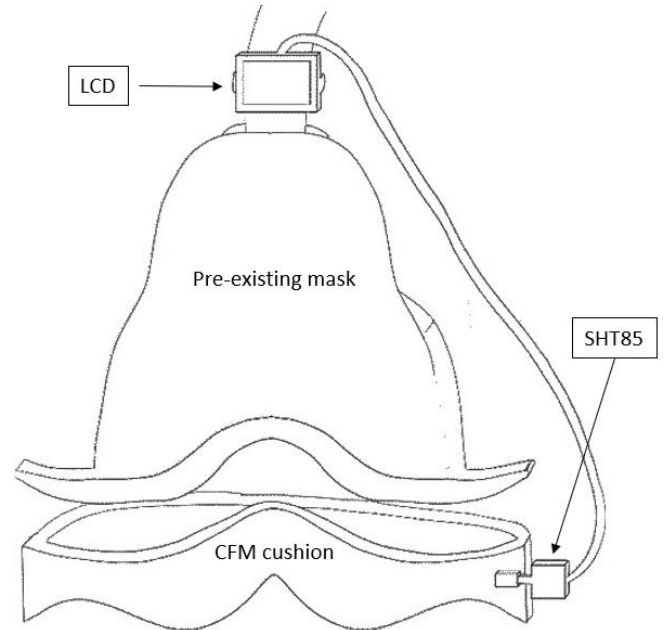
MeshLab, preparing it for 3D printing.

Fig. 2. The humidity and temperature sensor (SHT85) position at the skin-mask interface.

B. Microclimate Monitoring and Processing

The SHT85 sensor was used to collect data, which was then output to the LCD and, eventually, the PC by the electronic circuit (Fig. 3). The electronic system has been upgraded with a Bluetooth module to allow for continuous connectivity and the additional benefits of a wireless connection. The use of an Arduino Nano reduces the overall size of the device, and the circuit is powered by a Mini USB cable.

The data is processed in MATLAB and displayed as app. Threshold values were calculated independently in MATLAB and plotted on top of previous plots to show the dangerous level of T-H.
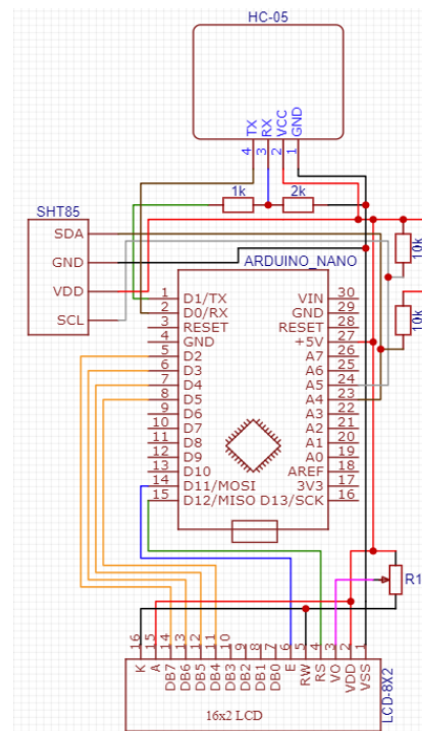

Fig. 3. Microclimate monitor circuit diagram.

With the addition of further features to the Arduino script, more useful data, such as dewpoint, could be displayed. A mask removal warning is also added, which is accomplished through the use of a small loop that compares recent decreases in the recorded values. An app created with App Inventor connects to the Nano due to the limited dimensions of the chosen LCD and the added functionality of the Bluetooth module. The app is used to inspect functional data such as generic plots, threshold labels, and mask removal warnings. If any of the fault conditions are met, the connected device vibrates.

C. Testing the Erythema Intensity of the CFM

A test is created to compare the erythema intensity of the CFM to that of the pre-existing mask, emphasizing comfort. Photos were taken in a controlled environment after 30 min of use on each mask (Fig. 4). These images were then evaluated using ImageJ, an image quantification software, followed by a MATLAB script. A simple visual inspection reveals that erythema is present on the original mask (Fig. 4(b)) in the previously mentioned bony prominence of the nasal bridge. In the CFM, however, erythema is less concentrated on the nasal ridge and spreads more evenly adjacent to the nose and infraorbital region (Fig. 4(c)).
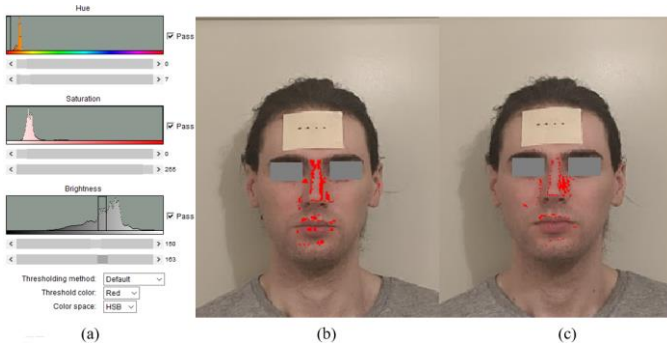

Fig. 4. Results of color thresholding using ImageJ, (a) Parameters (b) after original mask use (c) After CFM use.

III. RESULTS AND DISCUSSION

To evaluate the device's working principle, function tests are performed between both masks. As shown in Figs. 5 and Fig. 6, the CFM mask and the pre-existing mask were both equipped for 30 min while collecting data. There was a high level of robustness, and there were no significant issues with the monitors' ability to sample data. Before the final design was completed, any necessary changes were made in the appropriate programming code.

Initially, the device was tested by comparing the CFM and the original mask on a BWCT ventilator (SLE5000). This type of analysis would have required clinical conditions for the mask and sensory unit, including calibrated repeatability, consistent flow rate, and pressure. Furthermore, the device includes a leakage monitor, allowing leakage rates between masks to be compared. Because an external T-H unit controls each parameter in the ventilation circuit, T-H differences from the skin-mask could have been assessed, confirming the increase in surface moisture and skin temperature.

The images in Fig. 7 were evaluated using ImageJ, an image quantification software, followed by a MATLAB script. The results of color thresholding on ImageJ are shown in Fig. 4(b) and Fig. 4(c), where concentrated levels of red are

recognized around the top of the nose and less so in the CFM. Instead, after using CFM, a more extensive spread is seen to the right of the nose.
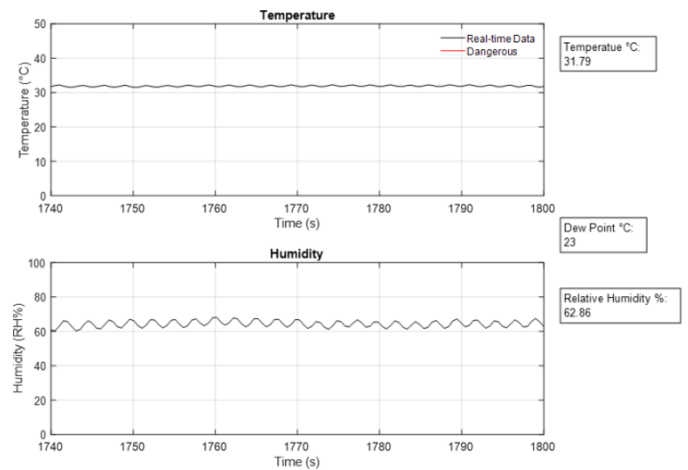

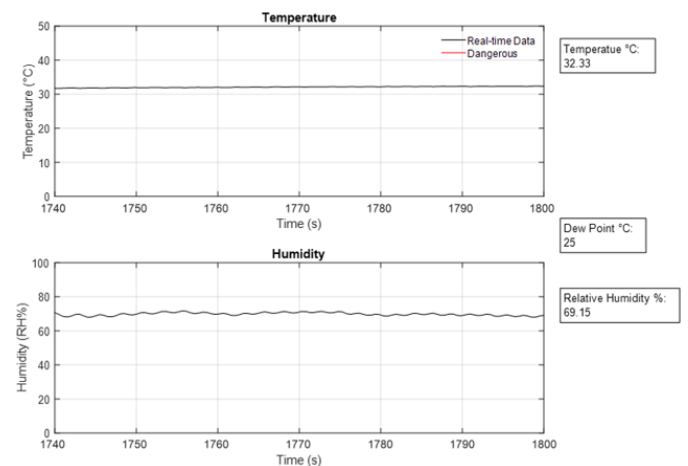Fig. 5. MATLAB App while performing initial monitor function test on CFM.

Fig. 6. MATLAB App while perfuming initial monitor function test on the pre-existing mask.

Again, this can be seen in the MATLAB results in Fig. 4(a), where blue and green are filtered out and only a small bandwidth of red is left; the resulting pixels are also blurred to aid in interpretation. As a result, this test can validate the improved pressure distribution from the CFM, reducing the load on the nasal bridge, where the thin skin is less likely to develop PUs.

Many methods were used to ensure repeatability when completing the erythema test. The camera is a Google Pixel smartphone mounted in a fixed position at eye level that did not move between tests. Each time, the subject is placed with their back to the wall, and tape on the floor ensures that the proper distance is maintained. Furthermore, the subject was shaved completely prior to data collection to ensure that all tissue was visible. As a reference for later processing, a piece of tape with four dots 1cm apart is placed on the subject's forehead. The photographs were taken in the same enclosed room under the same lighting conditions. Finally, the temperature for both sets of data is recorded within a tolerance of ±1 °C.

Due to the unique nature of the project, a sample size of one subject was used, and intersession tests helped prove the robustness. Multiple subjects would be preferable in a future

test to make accuracy comparisons. The subjects would be tested on the same equipment with identical settings during the previously mentioned ventilator tests.
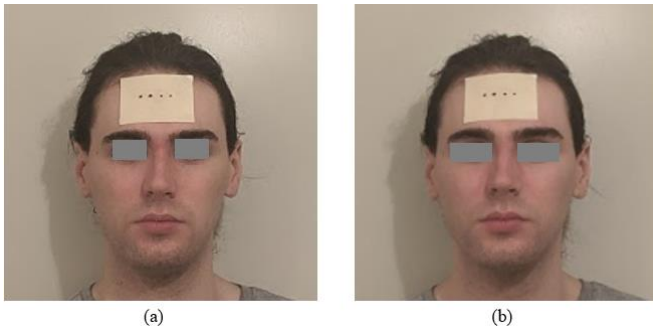

Fig. 7. Photos of the subject after original mask use (a) and CFM use (b).

Finally, all this functionality is combined into one single unit, and the fault conditions are shown in the MATLAB plots with an audible sound. All of the final design elements are integrated into two separate units, the monitor and the CFM, and the finished results are shown in Fig. 8.

The final prototype (Fig. 8) fulfilled the paper's initial goals. However, there is still room for improvement. The most important is to switch from the current Polylactic Acid (PLA) to a more clinically appropriate material like silicone. Silicone is commonly used in the medical industry because it is gentler on tissue and allows for some flexibility; additionally, unlike PLA, silicone is chemically inert and simple to decontaminate. Further advancements in 3D printing silicone could increase that potential.
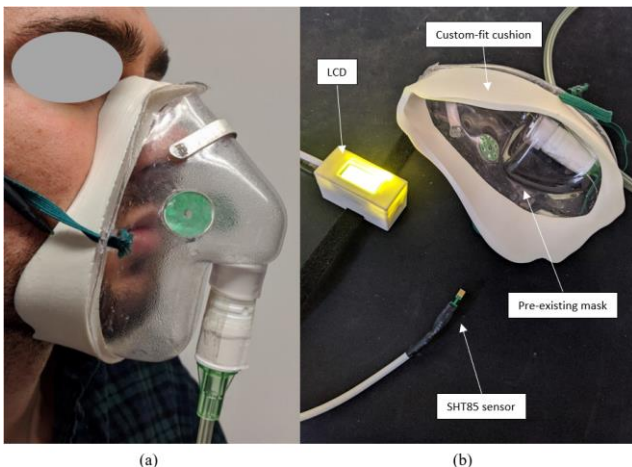

Fig. 8. The design of the CFM, a) CFM fitted to the Subject b) CFM hardware.

There were a few minor errors in the face mesh, mostly under the chin. To begin with, the Occipital 3D scanner used a small file size for the mesh and efficient but outdated scanning technology. Furthermore, because SolidWorks is not fully optimized for mesh files, creating a surface against the mesh is only a close approximation. As a result, Blender is recommended for further mesh file integration.

The strap is more stretched and applying excessive pressure because the patient-specific mask now has larger dimensions than before. By including a disposable adjustable strap in the design, the new strap could be more customizable for the patient while also being thicker and longer for added comfort.

In future developments, a method to keep the sensor in place will be required. The current small cut out does not provide sufficient grip on the sensor to keep it in place. Alternative methods, such as a sensor with an appropriately sized rubber seal, could help improve this. Similarly, a small latch could be printed on the outside edge to secure the sensor in the skin-mask interface.

IV. CONCLUSION

This study proposed a solution to reduce the generation of PUs while also monitoring the parameters that may generate PUs during treatment. A Custom-Fit Mask (CFM) was created and integrated with sensors to help reduce the impact of mask loading and monitor critical characteristics during Non-invasive Ventilation (NIV). Preliminary testing and validation indicate a promising outcome in terms of reducing and monitoring the impact of ventilation masks on the skin.

In the future, the microclimate sensor and CFM will be used in conjunction to determine optimal levels of humidity and temperature at the skin in order to prevent the development of pressure ulcers. In addition, implementation on patients who require long-term ventilation, where the benefits are greater.

CONFLICT OF INTEREST

The authors declare that they have no conflict of interest.

AUTHOR CONTRIBUTIONS

SM came up with the novel idea for this project, helped with the research, designed the mask, and wrote the paper. SL conducted the research, helped design the mask, and analyzed the data. All authors had approved the final version.

REFERENCES

[1] D. L. Lauderbaugh *et al.*, "Noninvasive ventilation device-related pressure injury in a children's hospital," *Respiratory Care*, vol. 64, no. 12, pp. 1455–1460, Dec. 2019.

[2] M. O. Visscher *et al.*, "Face masks for noninvasive ventilation: Fit, excess skin hydration, and pressure ulcers," *Respiratory Care*, vol. 60, no. 11, pp. 1536–1547, Sep. 2018.

[3] J. Apold and D. Rydrych, "Preventing device-related pressure ulcers," *Journal of Nursing Care Quality*, vol. 27, no. 1, pp. 28–34, Jan/Mar. 2012.

[4] P. Worsley, G. Prudden, G. Gower, and D. Bader, "Investigating the effects of strap tension during non-invasive ventilation mask application: A combined biomechanical and biomarker approach," *Med. Devices*, vol. 9, no. 12, pp. 409–417, Nov. 2016.

[5] A. Gefen, "How do microclimate factors affect the risk for superficial pressure ulcers: A mathematical modeling study," *J. Tissue Viability*, vol. 20, no. 3, pp. 81–88, Aug. 2011.

[6] L. C. Gerhardt, V. Strässle, A. Lenz, N. D. Spencer, and S. Derler, "Influence of epidermal hydration on the friction of human skin against textiles," *J. R. Soc. Interface*, vol. 5, no. 28, pp. 1317–1328, Nov. 2008.

[7] S. Yusuf, M. Okuwa, Y. Shigeta, M. Dai, T. Iuchi, S. Rahman, A. Usman, S. Kasim, J. Sugama, T. Nakatani, and H. Sanada, "Microclimate and development of pressure ulcers and superficial skin changes," *Int. Wound J.*, vol. 12, no. 1, pp. 40–46, Feb. 2015.

[8] W. Zhong, M. Xing, N. Pan, and H. Maibach, "Textiles and human skin, microclimate, cutaneous reactions: an overview," *Cutan Ocul Toxicol*, vol. 25, no. 1, pp. 23–39, Oct. 2008.

[9] M. Egawa, M. Oguri, T. Kuwahara, and M. Takahashi, "Effect of exposure of human skin to a dry environment," *Skin Res. Technol.*, vol. 8, no. 4, pp. 212–218, Nov. 2002.

[10] A. M. Esquinas Rodriguez, R. Scala, A. Soroksky, A. BaHammam, A. de Klerk, A. Valipour, D. Chiumello, C. Martin, and A. E. Holland "Clinical review: Humidifiers during non-invasive ventilation—Key topics and practical implications," *Critical Care*, vol. 16, no. 1, pp. 203–210, Feb. 2012.

[11] I. Yilmaz and U. Y. Gunes, "Sacral skin temperature and pressure ulcer development: A descriptive study," *Wound Manag Prev.*, vol. 65, no. 8, pp. 30–37, Aug. 2019.

[12] T. Tsuboi, M. Ohi, H. Kita, N. Otsuka, H. Hirata, T. Noguchi, K. Chin, M. Mishima, and K. Kuno, "The efficacy of a custom-fabricated nasal mask on gas exchange during nasal intermittent positive pressure ventilation," *Eur. Respir J.*, vol. 13, no. 1, pp. 152–156, Jan. 1999.

[13] C. Lanza, J. Arruda, A. Soares, M. Santos, A. Souza, L. Lanza, and A. Moreno, "Fabrication of a custom pediatric nasal mask for noninvasive ventilation using a maxillofacial elastomer: A straightforward technique," *J. Prosthet. Dent.*, vol. 121, no. 1, pp. 179–182, Jan. 2019.

[14] D. Han, J. Rhi, and J. Lee, "Development of prototypes of half-mask facepieces for Koreans using the 3D digitizing design method: A pilot study," *Ann. Occup. Hyg.*, vol. 48, no. 8, pp. 707–714, Oct. 2004.

[15] D. Hsu, Y. Cheng, M. Bien, and H. Lee, "Development of a method for manufacturing customized nasal mask cushion for CPAP therapy," *Australas Phys. Eng. Sci. Med.*, vol. 38, no. 4, pp. 657–664, Dec. 2015.

[16] Y. Wu, D. Acharya, C. Xu, B. Cheng, S. Rana, and K. Shimada, "Custom-fit three-dimensional-printed bipap mask to improve compliance in patients requiring long-term noninvasive ventilatory support," *J. Med. Device*, vol. 12, no. 3, pp. 0310031–310038, Sep. 2018.

[17] J. Kottner, J. Black, E. Call, A. Gefen, and N. Santamaria, "Microclimate: A critical review in the context of pressure ulcer prevention," *Clin Biomech*, vol. 59, pp. 62–70, Nov. 2018.

[18] H. Orsted and K. Harding, "Pressure ulcer prevention: pressure, shear, friction and microclimate in context," *International Review*, pp. 1–25, Sep. 2010.

[19] E. D. Bois, "The basal metabolism in fever," *J. Am. Med. Assoc*, vol. 77, no. 5, pp. 352–357, Jul. 1921.

[20] D. Chiumello, "Is humidification always necessary during noninvasive ventilation in the hospital?" *Respir Care*, vol. 55, no. 7, 950, Jul. 2010.

[21] K. A. Engebretsen, J. D. Johansen, S. Kezic, A. Linneberg, and J. P. Thyssen, "The effect of environmental humidity and temperature on skin barrier function and dermatitis," *J. Eur. Acad. Dermatol Venereol*, vol. 30, no. 2, pp. 223–249, Feb. 2016.

[22] J. Alqahtani, P. Worsley, and D. Voegeli, "Effect of humidified noninvasive ventilation on the development of facial skin breakdown," *Respir Care*, vol. 63, no. 9, pp. 1102–1110, Sep. 2018.

[23] N. Kramer, T. Meyer, J. Meharg, R. Cece, and N. Hill, "Randomized, prospective trial of noninvasive positive pressure ventilation in acute respiratory failure," *Am. J. Respir Crit. Care Med.*, vol. 151, no. 6, pp. 1799–1806, Jun. 1995.

[24] B. Schönhofer and S. Sortor-Leger, "Equipment needs for noninvasive mechanical ventilation," *Eur. Respir J.*, vol. 20, no. 4, pp. 1029–1036, Oct. 2020.

[25] P. Navalesi, F. Fanfulla, P. Frigerio, C. Gregoretti, and S. Nava, "Physiologic evaluation of noninvasive mechanical ventilation delivered with three types of masks in patients with chronic hypercapnic respiratory failure," *Crit. Care Med.*, vol. 28, no. 6, pp. 1785–1790, Jun. 2000.

[26] H. Kwok, J. McCormack, R. Cece, J. Houtchens, and N. Hill, "Controlled trial of oronasal versus nasal mask ventilation in the treatment of acute respiratory failure," *Crit. Care Med.*, vol. 31, no. 2, pp. 468–473, Feb. 2003.